Supporting Information

Pure hydrophilic block copolymer vesicles with redox- and pH-cleavable crosslinks

Jochen Willersinn,[†] *Bernhard V.K.J. Schmidt*[†*]

[†] Max-Planck Institute of Colloids and Interfaces; Department of Colloid Chemistry, Am Mühlenberg 1, 14476 Potsdam, Germany

Bernhard.schmidt@mpikg.mpg.de

Depolymerization of pullulan: Pullulan was depolymerized according to a procedure reported in literature.[1] In a dry, argon purged 100 mL round bottom Schlenk flask commercially available pullulan (4.0 g) was dissolved in aqueous hydrochloric acid solution (80 mL, 0.025 mol·L^{-1}). The flask was sealed and immersed in a pre-heated oil bath at 85 °C. The solution was stirred for 2.5 h and the depolymerization reaction was stopped by putting the flask into an ice bath. The cooled reaction mixture was placed in a 10 000 MWCO dialysis tube and extensively dialyzed against deionized water for three days. The solution was lyophilized to afford depolymerized pullulan as colorless solid (3.0 g, 75% recovery, $M_{\mathrm{n,SEC}}$ = 22 400 g·mol^{-1}, pullulan standard in acetate buffer with 20% MeOH, $Đ = 1.8$)

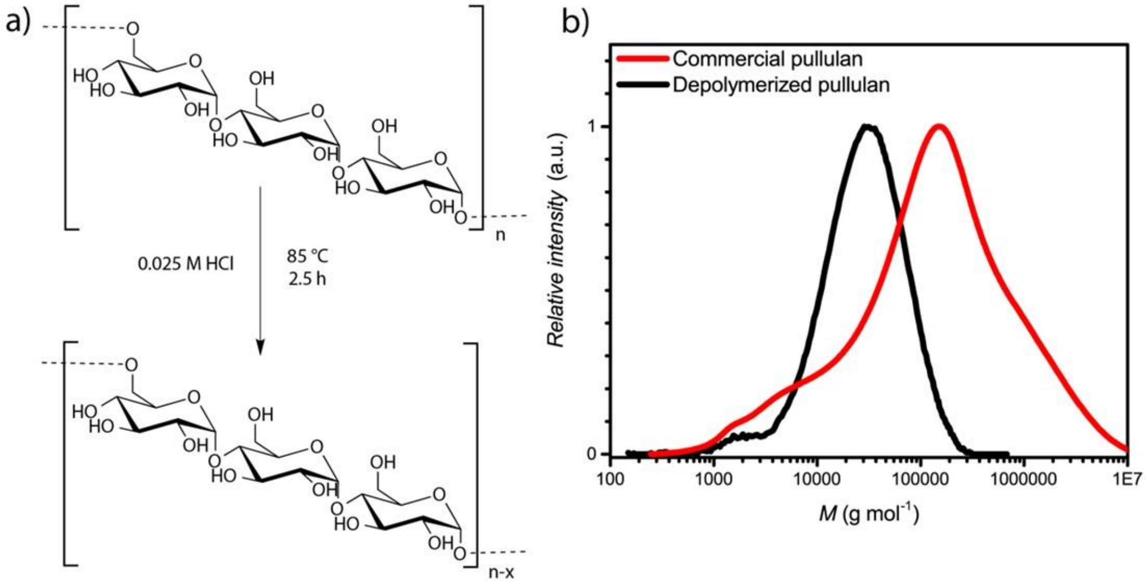

Figure S1. a) Reaction scheme of pullulan depolymerization; b) apparent molecular mass distributions of commercial pullulan and depolymerized pullulan against a pullulan calibration curve determined *via* SEC in acetate buffer solution.

Amino functionalization of pullulan (Pull-NH$_2$): Amino terminated pullulan was synthesized according to a derived procedure reported by Schatz et. al.[2] In a dry, argon purged 100 mL round bottom Schlenk flask pullulan (2.5 g, 0.112 mmol, 1 eq.) was dissolved in acetate buffer solution

(75 mL, 50 mM). Hexamethylene diamine (1.30 g, 11.16 mmol, 100 eq.) was added and the flask was immersed into a pre-heated oil bath at 50 °C. Sodium cyanoborohydride (0.175 g, 2.79 mmol, 25 eq.) was added and the mixture was stirred for 96 hours with a repeated daily addition of sodium cyanoborohydride. The reaction mixture was intensively dialyzed against deionized water (SpectraPor 3.5 kD MWCO tube) for three days and lyophilized to afford amino terminated pullulan (Pull-NH$_2$) (2.45 g, 98% recovery, $M_{\mathrm{n,SEC}}$ = 16 100 g·mol^{-1}, pullulan standard in acetate buffer with 20% MeOH, $Đ$ = 1.8). The full conversion was confirmed by the disappearance of the anomeric proton signals of the reducing group in the ^{1}H-NMR spectrum (400 MHz, DMSO-d$_6$, 6.67 ppm and 6.32 ppm).

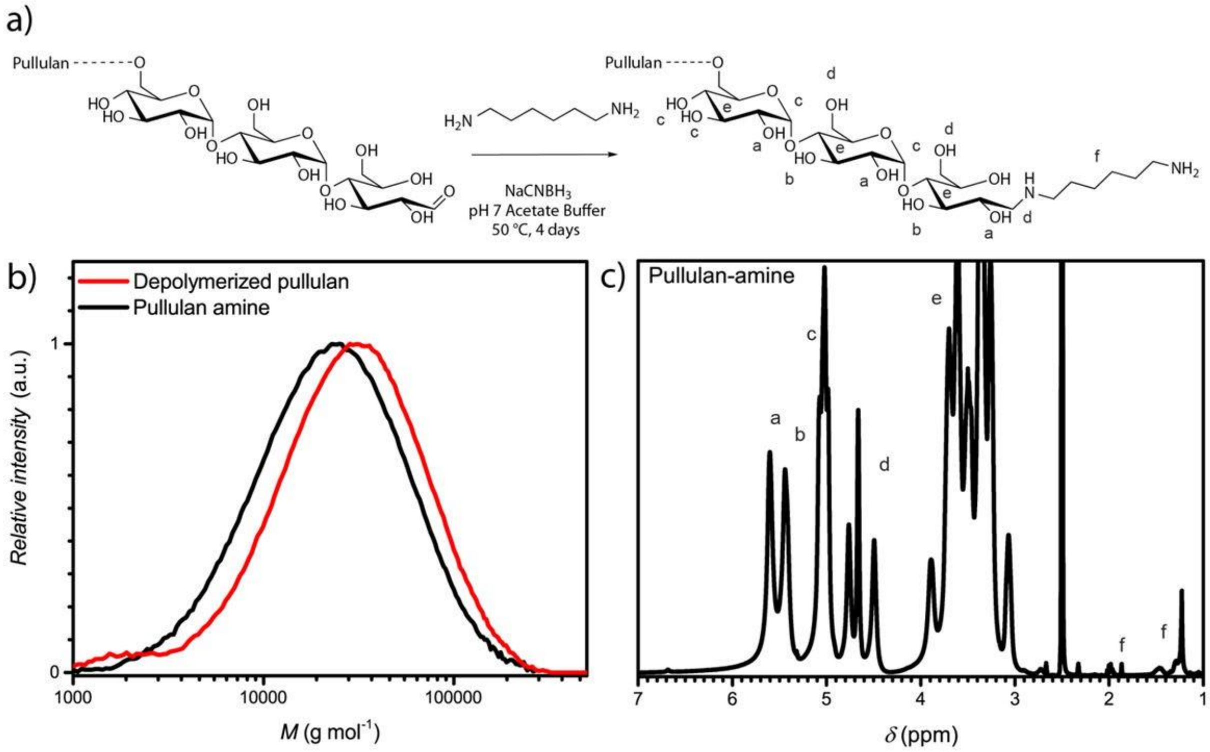

Figure S2. a) Reductive amination scheme of pullulan with hexamethylenediamine; b) apparent molecular mass distributions of depolymerized pullulan and amine functionalized pullulan against a pullulan calibration curve determined *via* SEC in acetate buffer solution; c) corresponding ^{1}H-NMR of pullulan amine recorded at 400 MHz in DMSO-d$_6$.

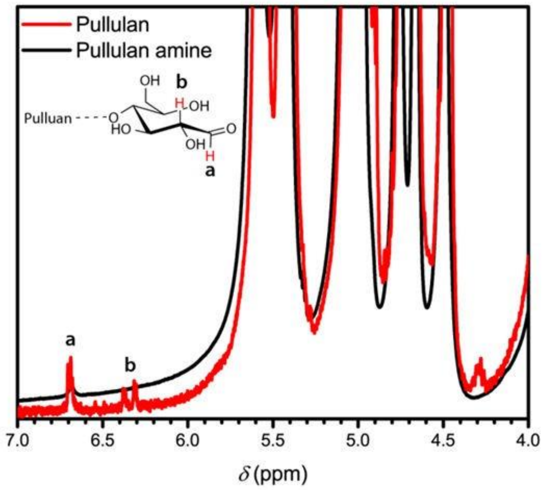

Figure S3. ^{1}H-NMR comparison of depolymerized pullulan and amine functionalized pullulan recorded at 400 MHz in DMSO-d_6 displaying the disappearance of the anomeric proton signals.

2,5-dioxopyrrolidin-1-yl 2-bromopropanoate:[3] In a dry, argon purged 250 mL three neck round bottom flask with condenser and addition funnel *N*-hydroxysuccinimide (4.0 g, 34.75 mmol, 1.2 eq.) was dissolved in dry dichloromethane (70 mL). Dry pyridine (2.57 mL 31.85 mmol, 1.1 eq.) was added and the reaction mixture was cooled to 0 °C. The addition funnel was charged with a mixture of 2-bromopropionylbromide (3.10 mL, 29.58 mmol, 1.0 eq.) and dry DCM (35 mL) under argon flow. The mixture was added dropwise to the reaction within 30 minutes. The reaction was allowed to warm to ambient temperature and stirred for 18 hours. Afterwards, DCM (70 mL) was added. The organic phase was washed with 1M aqueous HCl solution (4 x 70 mL), deionized water (1 x 100 mL), saturated aqueous brine solution (1 x 100 mL) and dried over anhydrous magnesium sulfate. The solvent was removed in vacuum to afford 2,5-dioxopyrrolidin-1-yl 2-bromopropanoate (6.5 g, 29.41 mmol, 99% yield). ^{1}H NMR (400 MHz, $CDCl_3$, δ:) 4.61 (q, ^{3}J = 7.0 Hz, 1H, *CH*), 2.85 (t, ^{3}J = 19.2 Hz, 4H, CH_2), 1.95 (d, ^{3}J = 7.0 Hz, 3H, CH_3).

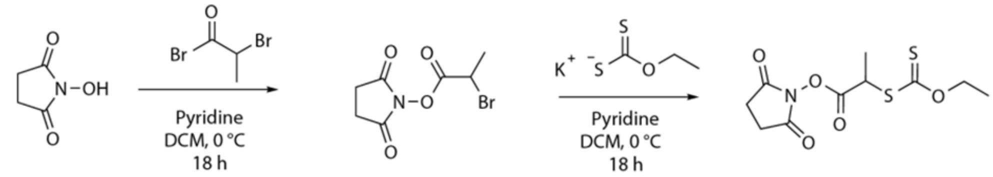

Scheme S1. Schematic synthesis of the *N*-succinimidyl xanthate.

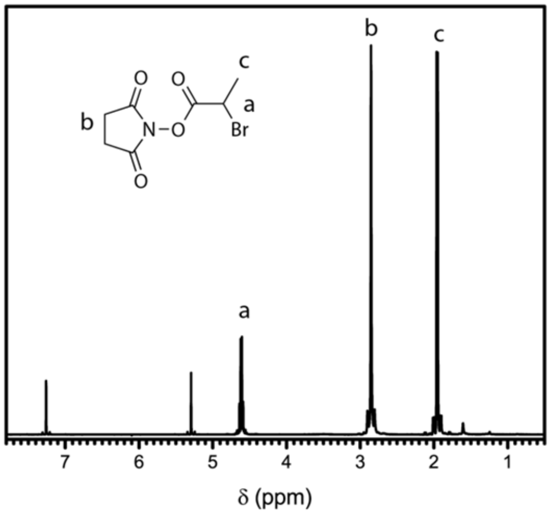

Figure S4. ^{1}H NMR of 2,5-dioxopyrrolidin-1-yl 2-bromopropanoate recorded at 400 MHz in $CDCl_3$.

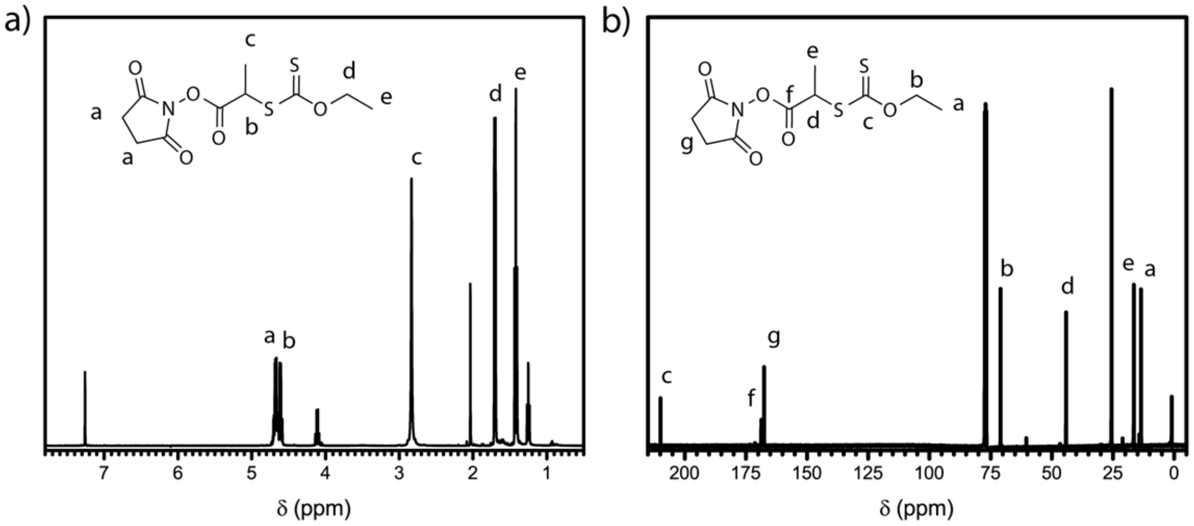

Figure S5. a) ^{1}H-NMR of 2,5-dioxopyrrolidin-1-yl 2-((ethoxycarbonothioyl)thio)propanoate in $CDCl_3$ at 25 °C; b) ^{13}C-NMR of 2,5-dioxopyrrolidin-1-yl 2-((ethoxycarbonothioyl)thio)propanoate in $CDCl_3$ at 25 °C.

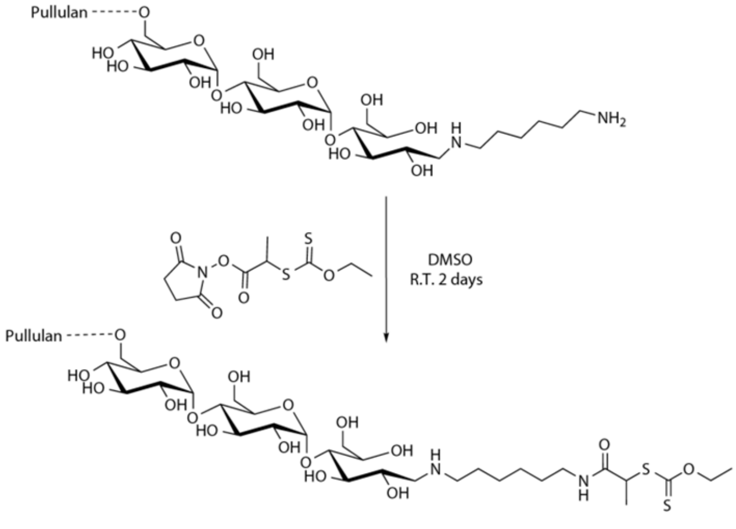

Scheme S2. Schematic transfer of the xanthate group to pullulan amine.

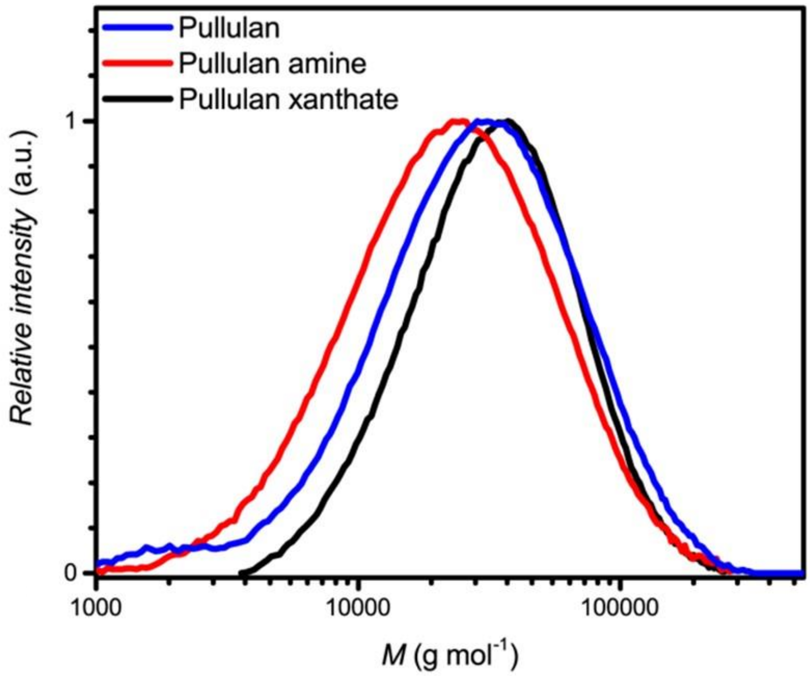

Figure S6. Apparent molecular mass distributions of the reaction cascade of pullulan recorded *via* SEC in acetate buffer against a pullulan calibration curve.

Table S1. Summary of SEC results of the pullulan functionalization recorded in acetate buffer against a pullulan calibration curve.

Polymer	$M_{n,app,SEC}$ (g·mol^{-1})	*Đ*
Pullulan	22 000	2.0
Pullulan amine	16 000	2.1
Pullulan xanthate	26 500	1.7

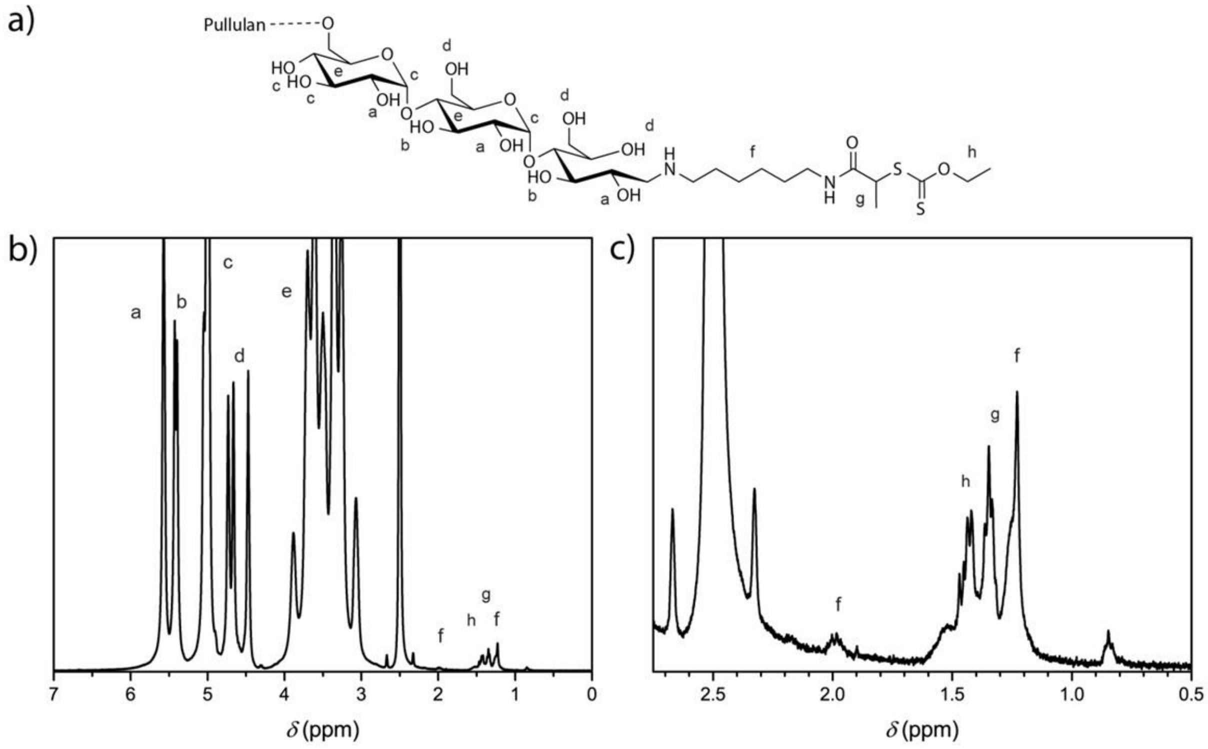

Figure S7. a) Scheme of pullulan xanthate; b) ^{1}H-NMR spectrum of pullulan xanthate and c) a magnification of the location corresponding to the protons of the functional group recorded at 400 MHz in DMSO-d$_6$.

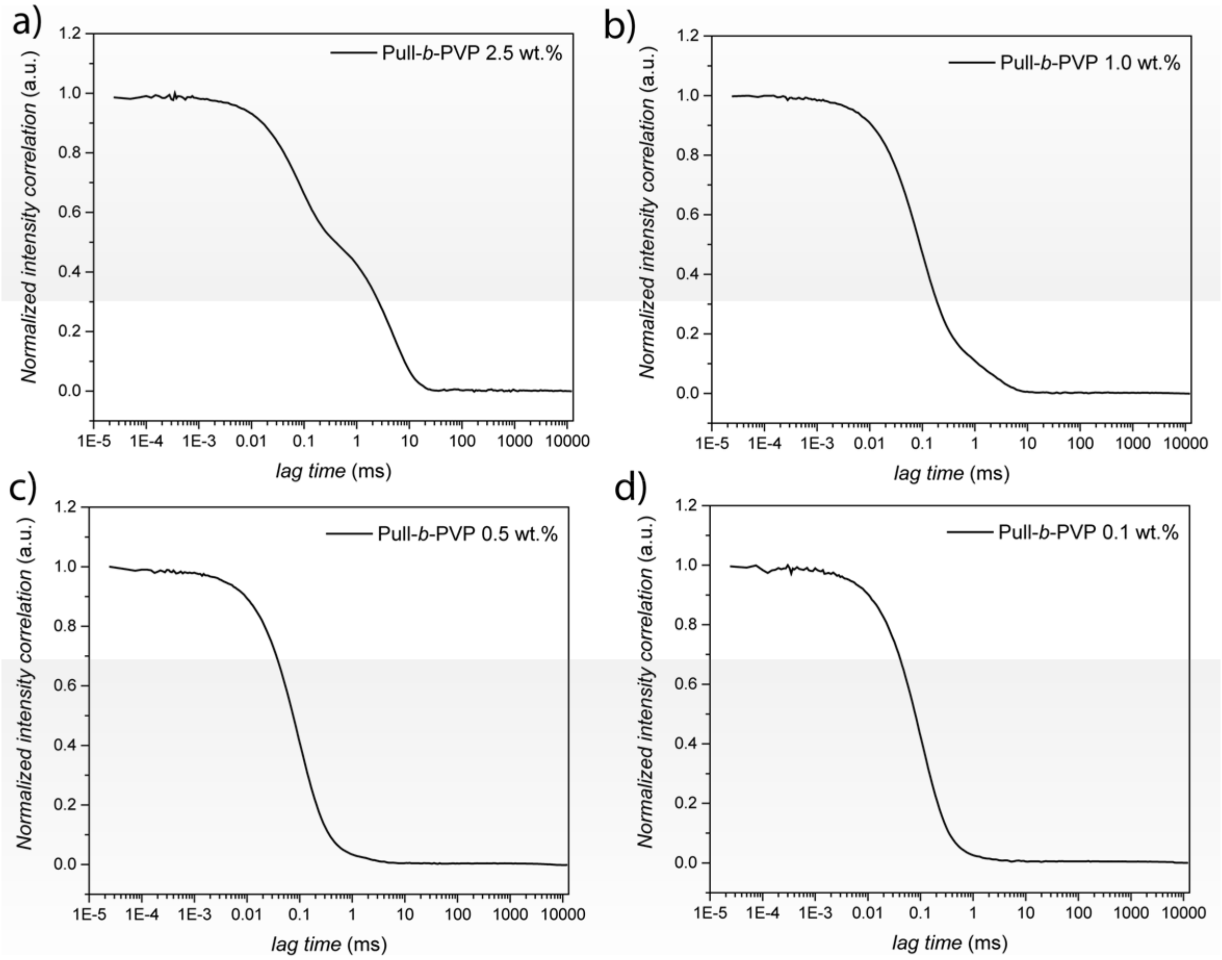

Figure S8. Intensity correlation data of Pull_{124}-*b*-PVP_{263} block copolymer in Millipore water measured *via* DLS at 25 °C.

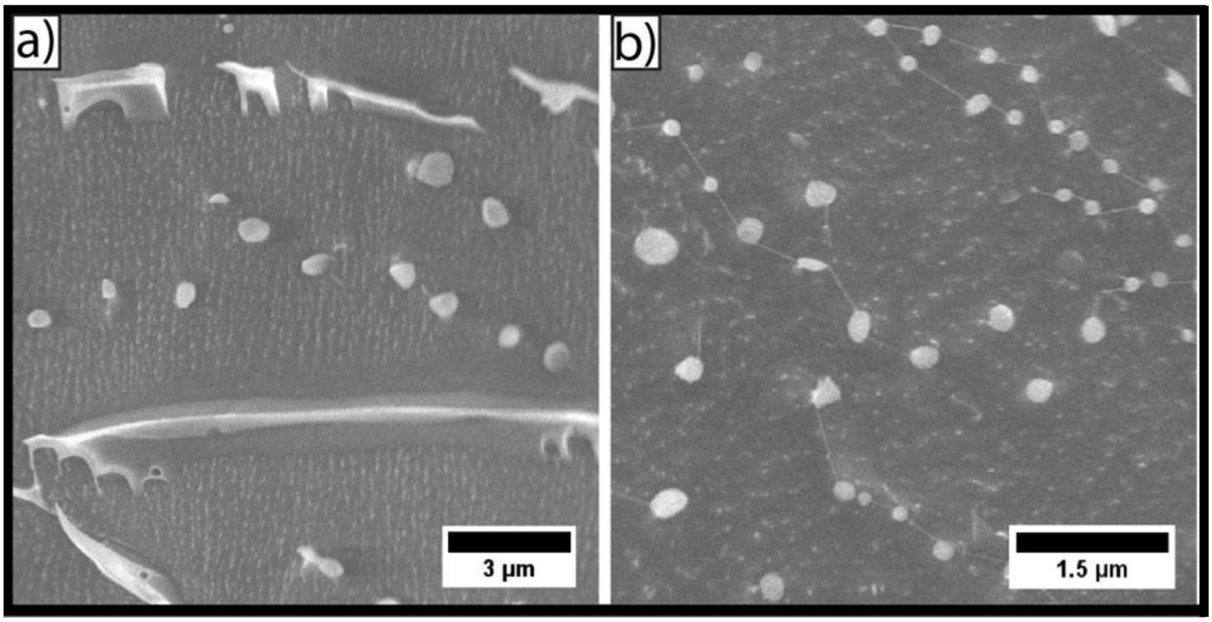

Figure S9. Cryogenic SEM micrographs of a 0.5 wt.% Pull$_{124}$-*b*-PVP$_{263}$ solution displaying spherical particles and tubular alignments of free dissolved block copolymer due to the formation of ice crystals during the preparation process.

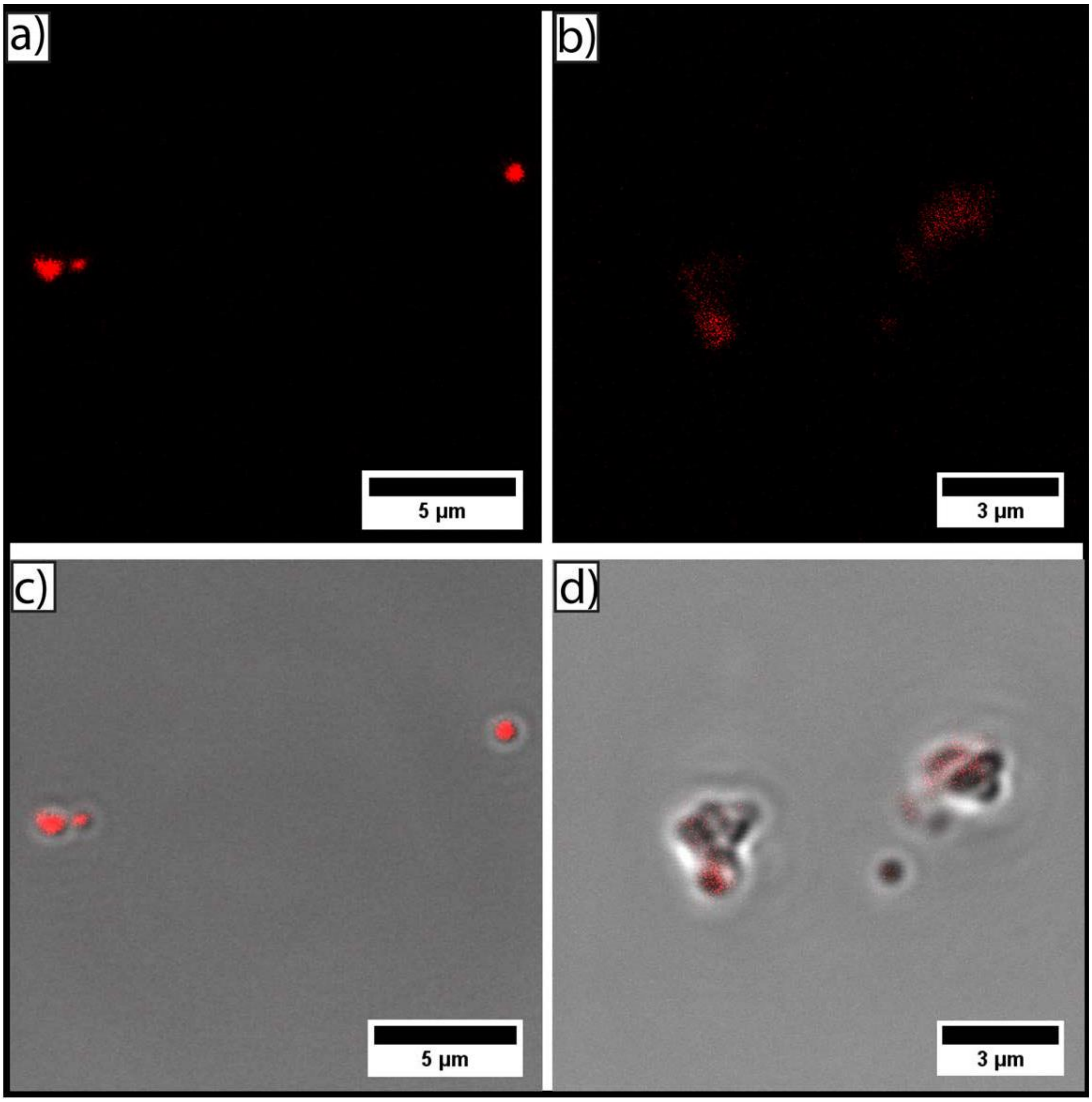

Figure S10. a), b) Confocal micrographs of spherical particles of Pull-*b*-PVP at 2.5 wt.% stained with 0.08 mM Rhodamine B; c), d) corresponding DIC images with fluorescence overlay displaying the particle structure.

Selective oxidation of pullulan

The synthesis was performed according to a procedure reported by Maia et al.[4] The following procedure is exemplified for an oxidation of 5%. The corresponding data for higher oxidations can be obtained from Table S2.

In a 50 mL round bottom flask, pullulan (2.0 g, 0.14 mmol) was dissolved in deionized water (32 mL) to afford a 12.5 wt.% solution. The solution was separated into 6 parts containing 5 mL of the pullulan solution. Subsequently, an aqueous solution of $NaIO_4$ (0.032 g, 0.15 mmol in 1 mL deionized water) was added to the pullulan sample and the reaction mixture was stirred for 20 hours at room temperature. Diethylene glycol (14 µL, 0.015 mmol) was added and the reaction mixture was stirred 1 hour, followed by dialysis and lyophilization to afford 5% oxidized pullulan (0.275 g, 0.017 mmol) as a white powder. $M_{n,SEC}$ = 14 100 g·mol^{-1}, pullulan standard in acetate buffer with 20% MeOH, $Đ$ = 2.1.

The state of oxidation was characterized *via* ^{1}H-NMR spectroscopy. Furthermore, SEC measurements should indicate possible depolymerization or degradation of oxidized pullulan. As shown in the ^{1}H-NMR spectra in Figure S10b, new signals are arising in the area between 6.1 ppm and 7.5 ppm which increase in intensity and the area below the curve with increasing theoretical oxidation state. These peaks can be attributed to the increasing number of aldehydes formed by the oxidation of a hexose to a dialdehyde. In parallel to the increase in aldehyde peaks, the signals corresponding to the hydroxyl groups and the α-3-centered protons between 4.5 ppm and 5.6 ppm decrease significantly with increasing amount of oxidized glucose units. The ^{1}H-NMR affords a qualitative measure for the increasing amount of oxidized groups, but in order to quantify the amount of aldehydes an internal standard had to be applied. Therefore, 0.013 mmol DMF was added to a solution of 0.005 g of oxidized pullulan in 0.7 mL DMSO-d_6. The low amount of DMF should ensure a distinguishable proton signal which can be used as an internal standard peak. DMF was chosen because of the singlet amide proton signal in a chemical region, where no signals from pullulan and its oxidized species occur. The corresponding amide peak at 8.0 ppm was integrated, normalized to one, and the area below the signals between 6.1 ppm and 7.5 ppm was integrated.

The integral of the 0% oxidation was set to be 1 oxidized unit (ω-aldehyde) and the oxidized glucose were calculated from integrals corresponding to higher oxidations as follows. With an apparent average number weighted molecular weight of 14 400 $g \cdot mol^{-1}$, the non-oxidized pullulan possesses approximately 80 glucose units. This pullulan already features one aldehyde group at its terminal glucose unit with an integral of 0.42 in correspondence to the integral of the internal standard. By relating the integrals of higher theoretical oxidations with these values, the number of oxidized units can be determined (Table S3). The line graph in Figure S10c displays a linear increase in oxidized units with increasing theoretical oxidation. However, the increase becomes less predominant for theoretical oxidations above 25%. Whereas the actual oxidation matches quite nicely with the theoretical one for attempted oxidations below 25%, higher oxidized samples do show significant discrepancies, i.e. the actual percentage is significantly lower than the theoretical one.

The decrease in oxidized groups with increasing amount of $NaIO_4$ can be explained by taking the SEC elution curves in Figure S11 into account. As visible from the elution curves in Figure S11a, the elution curves shift to a higher elution volume upon increasing oxidation indicating a decrease in the size of the pullulan. The apparent average molecular weight distribution in Figure

S11b further states this observation leading to the assumption that pullulan fractures upon higher oxidation.

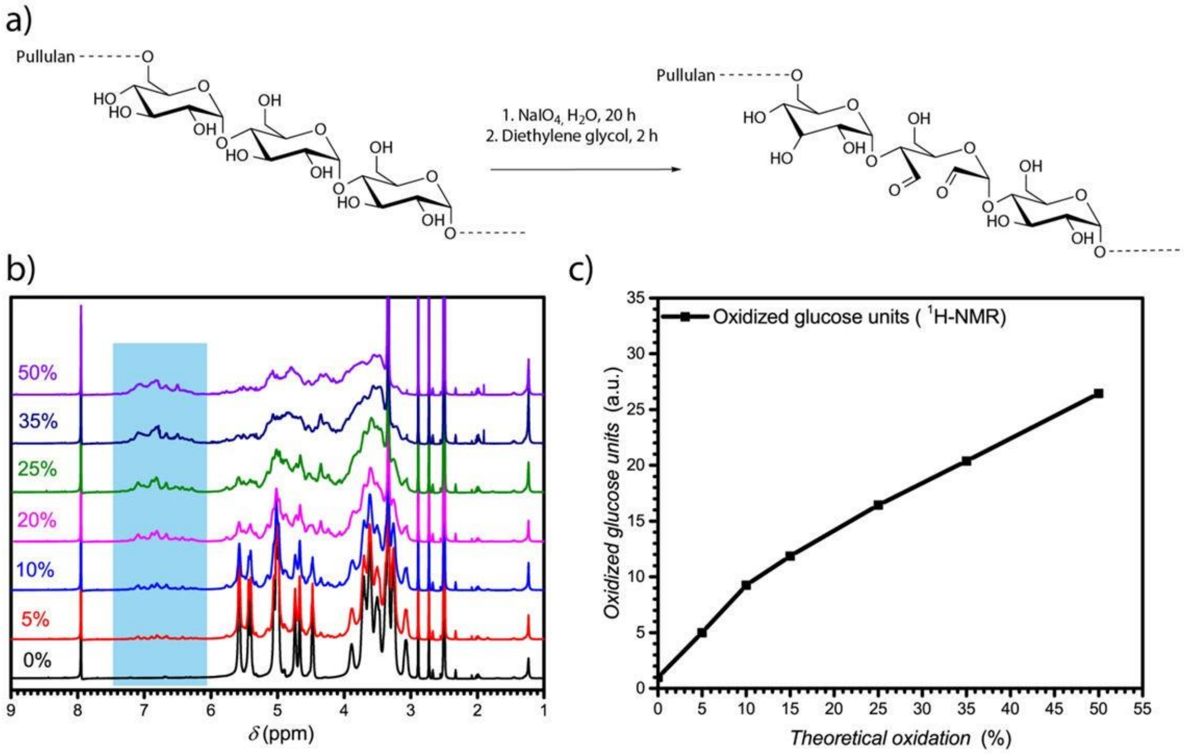

Figure S11. a) Schematic oxidation of pullulan with $NaIO_4$; b) ^{1}H-NMR spectra of oxidized pullulans emphasizing on the anomeric proton peaks of the oxidized glucose units recorded at 400 MHz in DMSO-d_6; c) line plot of oxidized pullulan units against the theoretical oxidation.

Table S2. Assessment and SEC results of the pullulan oxidation with $NaIO_4$.

Oxidation (%)	***m*** **($NaIO_4$) (g)**	***V*** **(DEG) (µL)**	***m*** **(Pull) (g)**	***n*** **(Pull) (mmol)**	**$M_{n,SEC}$ g·mol^{-1}**
5	0.032	14	0.275	0.017	16 100
10	0.064	28	0.284	0.02	14 400
15	0.128	56	0.289	0.017	16 600
25	0.160	70	0.275	0.021	13 200
35	0.224	98	0.239	0.016	14 800
50	0.320	140	0.252	0.026	9 600

Table S3. Summary of ^{1}H-NMR oxidation experiments of a pullulan homopolymer.

Theoretical oxidation (%)	**Integral**	**Oxidized units**	**Oxidation (%)**
0	0.42	1	1
5	2.12	5	6.3
10	3.89	9.3	11.6
15	4.98	11.9	14.8
25	6.91	16.5	20.6
35	8.56	20.4	25.5
50	11.11	26.5	33.1

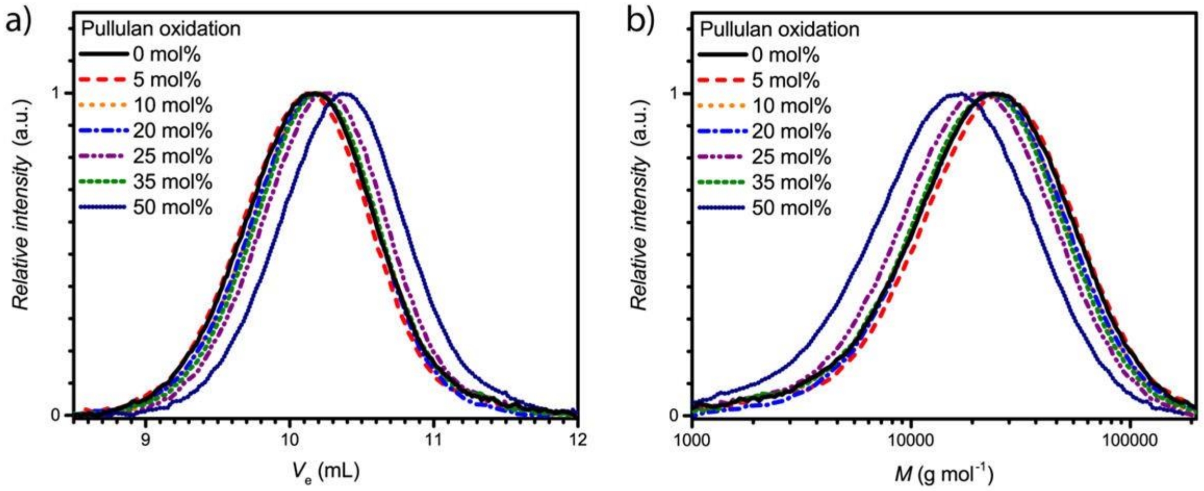

Figure S12. a) SEC traces of oxidized pullulan at different oxidation percentages and b) corresponding apparent molecular weight distributions recorded in acetate buffer solution against a pullulan calibration curve.

Table S4. Summary of DLS results of the oxidation, crosslinking and disassembly of Pull-*b*-PVP at 0.1 wt.%.

Polymer	**Peak 1 $R_{h,app}$ (nm)**	**Rel. abund.**	**Peak 2 $R_{h,app}$ (nm)**	**Rel. abund.**
Pull-*b*-PVP 5% oxidized	13	1.0	160	0.8
Pull-*b*-PVP crosslinked	14	0.2	340	1.0
Pull-*b*-PVP after TCEP addition	14	0.92	240	1.0
Pull-*b*-PVP after HCL addition	15	0.77	250	1.0

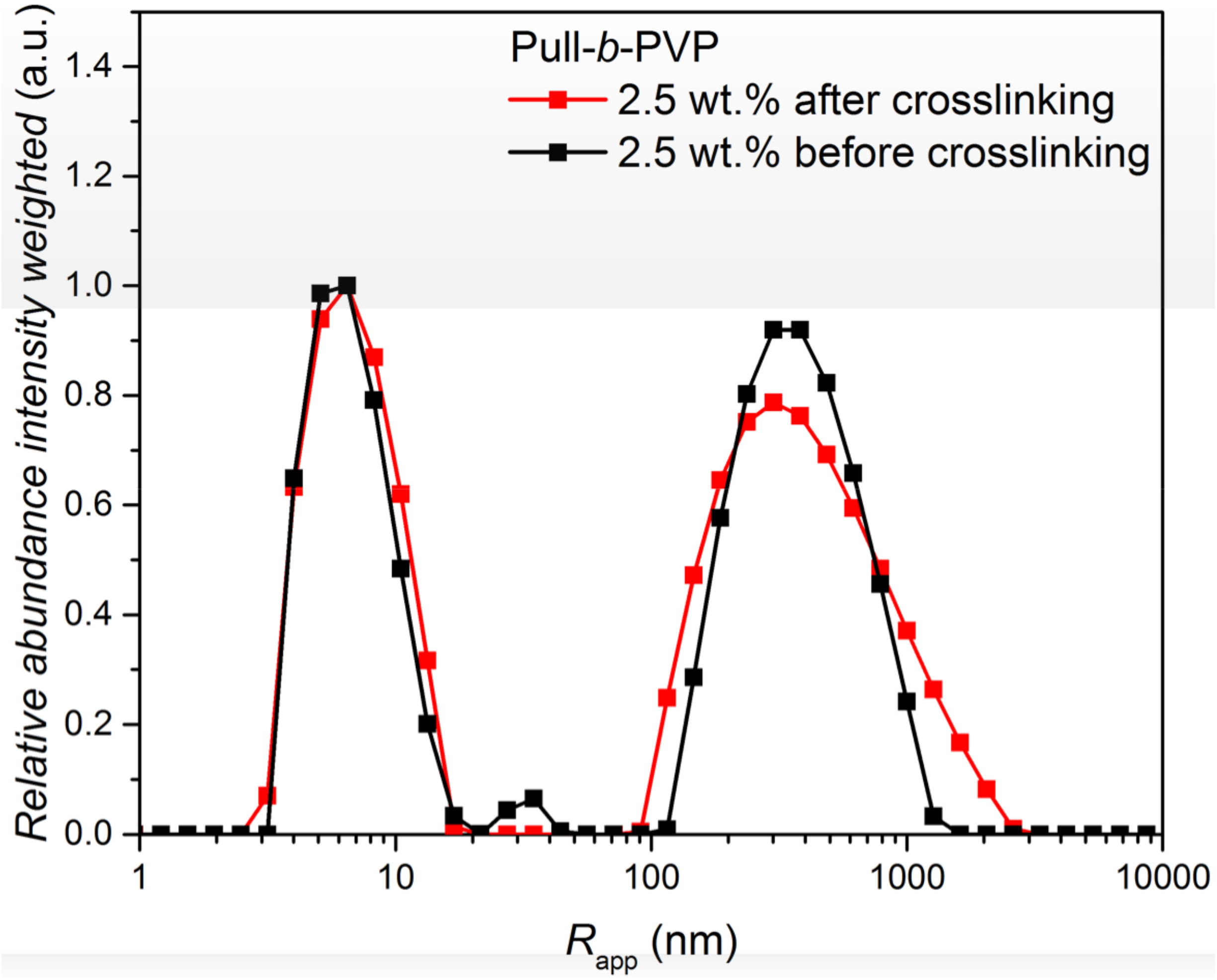

Figure S13. Intensity weighted particle size distributions of 2.5 wt.% solutions of Pull_{124}-*b*-PVP_{263} oxidized block copolymer before and after crosslinking with 10% of oxidized pullulan in Millipore water measured *via* DLS at 25 °C.

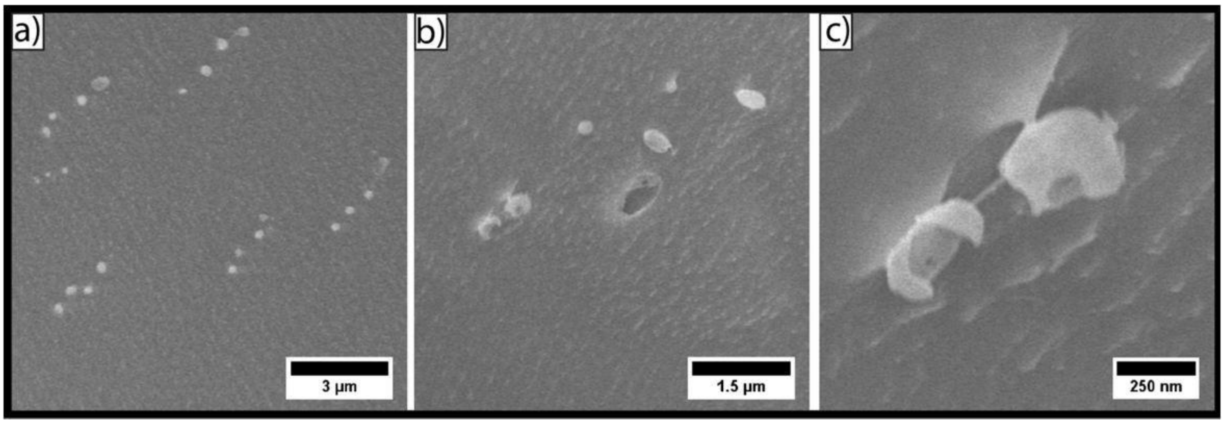

Figure S14. Cryo SEM micrographs of 5% oxidized Pull-*b*-PVP particles after crosslinking and dialysis displaying a) spherical particles and b) & c) hollow vesicular structures of with different diameters.

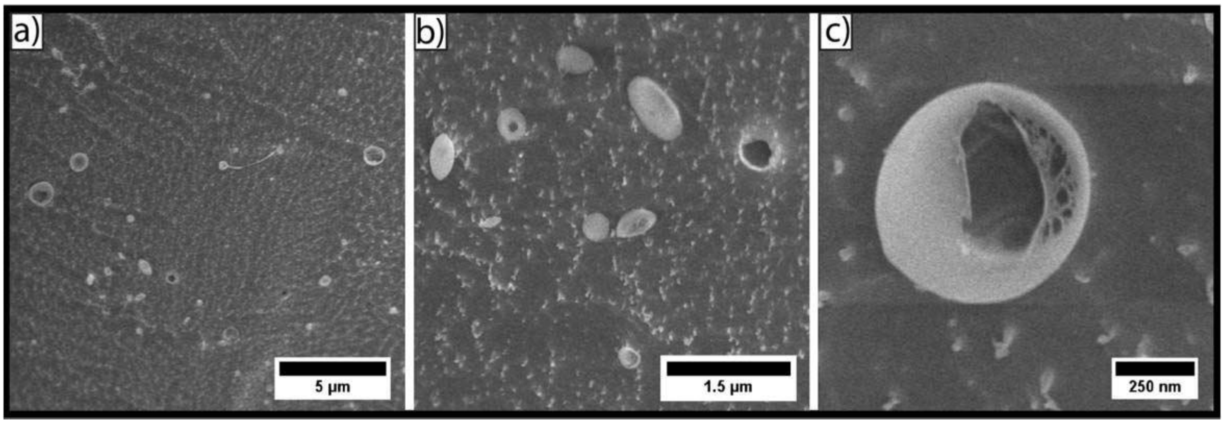

Figure S15. Cryo SEM micrographs of 10% oxidized Pull-*b*-PVP particles after crosslinking and dialysis displaying a) spherical vesicular structures and a minor amount of small spherical particles; b) & c) a magnification of a crosslinked Pull-*b*-PVP vesicle.

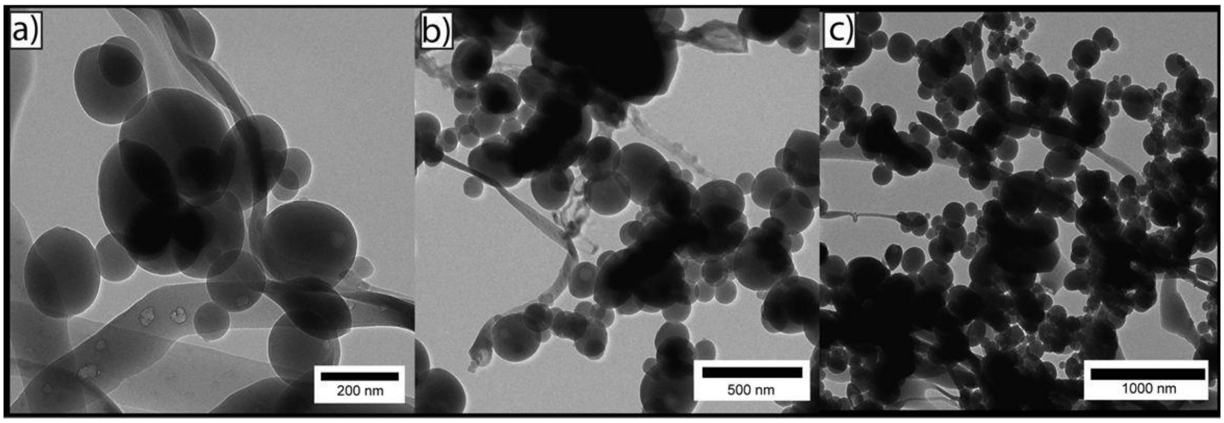

Figure S16. TEM images of 10% oxidized Pull_{124}-*b*-PVP_{263} after crosslinking and freeze drying on a copper grid.

References:

1 Ilić, L.; Jeremić, K.; Jovanović, S. Kinetics of pullulan depolymerization in hydrochloric acid. *Eur. Polym. J.* **1991,** 27 (11), 1227-1229.

2 Schatz, C.; Louguet, S.; Le Meins, J.-F.; Lecommandoux, S. Polysaccharide-block-polypeptide Copolymer Vesicles: Towards Synthetic Viral Capsids. *Angew. Chem., Int. Ed.* **2009,** 48 (14), 2572-2575.

3 Lecolley, F.; Tao, L.; Mantovani, G.; Durkin, I.; Lautru, S.; Haddleton, D. M. A new approach to bioconjugates for proteins and peptides ("pegylation") utilising living radical polymerisation. *Chem. Commun.* **2004,** (18), 2026-2027.

4 Maia, J.; Ferreira, L.; Carvalho, R.; Ramos, M. A.; Gil, M. H. Synthesis and characterization of new injectable and degradable dextran-based hydrogels. *Polymer* **2005,** 46 (23), 9604-9614.